Macromolecules
ARTICLE

Macromolecules **2010**, *43*, 811–820 **811**
DOI: 10.1021/ma902241b

Donor−Acceptor Polymers Incorporating Alkylated Dithienylbenzothiadiazole for Bulk Heterojunction Solar Cells: Pronounced Effect of Positioning Alkyl Chains

Huaxing Zhou,[†] Liqiang Yang,[‡] Shengqiang Xiao,[†,§] Shubin Liu,[⊥] and Wei You*[,†]

[†]*Department of Chemistry, University of North Carolina at Chapel Hill, Chapel Hill, North Carolina 27599-3290,* [‡]*Curriculum in Applied Sciences and Engineering, University of North Carolina at Chapel Hill, Chapel Hill, North Carolina 27599-3287,* [§]*State Key Lab of Advanced Technology for Materials Synthesis and Processing, Wuhan University of Technology, Wuhan, P. R. China 430070, and* [⊥]*Research Computing Center, University of North Carolina at Chapel Hill, Chapel Hill, North Carolina 25599-3420*

Received October 8, 2009; Revised Manuscript Received November 24, 2009

ABSTRACT: 4,7-Di(thiophen-2-yl)benzothiadiazole (**DTBT**) has been used to construct a number of donor−acceptor low band gap polymers for bulk heterojunction (BHJ) photovoltaics with high efficiency numbers. Its strong tendency to π-stack often leads to polymers with low molecular weight and poor solubility, which could potentially be alleviated by anchoring solubilizing chains onto the **DTBT** unit. A systematic study of the effect of positioning alkyl chains on **DTBT** on properties of polymers was implemented by investigating a small library of structurally related polymers with identical conjugated backbone. This series of donor−acceptor polymers employed a common donor unit, benzo[2,1-*b*:3,4-*b*′]dithiophene (**BDT**), and modified **DTBT** as the acceptor unit. Three variations of modified **DTBT** units were prepared with alkyl side chains at (a) the 5- and 6-positions of 2,1,3-benzothiadiazole (**DTsolBT**), (b) 3-positions of the flanking thienyl groups (**3DTBT**), and (c) 4-positions (**4DTBT**), in addition to the unmodified **DTBT**. Contrary to results from previous studies, optical and electrochemical studies disclosed almost identical band gap and energy levels between **PBDT−4DTBT** and **PBDT−DTBT**. These results indicated that anchoring solubilizing alkyl chains on the 4-positions of **DTBT** only introduced a minimum steric hindrance within **BDT−DTBT**, maintaining the extended conjugation of the fundamental structural unit (**BDT−DTBT**). More importantly, the additional high molecular weight and excellent solubility of **PBDT−4DTBT** led to a more uniform mixture with PCBM, with better control on the film morphology. All these features of **PBDT−4DTBT** led to a significantly improved efficiency of related BHJ solar cells (up to 2.2% has been observed), triple the efficiency obtained from BHJ devices fabricated from the "conventional" **PBDT−DTBT** (0.72%). Our discovery reinforced the importance of high molecular weight and good solubility of donor polymers for BHJ solar cells, in addition to a low band gap and a low HOMO energy level, in order to further enhance the device efficiencies.

Introduction

In recent years there has been tremendous progress in the field of bulk heterojunction (BHJ) polymer solar cells since its inception in 1995.[1] The overall energy conversion efficiency has been steadily improving from an initial 1% via a blend of poly[2-methoxy-5-(3′,7′-dimethyloctyloxy)-1,4-phenylenevinylene] (MDMO-PPV) with [6,6]-phenyl C_{60}-butyric acid methyl ester (PCBM)[2] to an impressive ∼5% achieved by poly(3-hexylthiophene) (P3HT):PCBM via extensive morphology optimization.[3−5] In order to further improve the efficiency of BHJ polymer solar cells, the research community is enthusiastically searching for new polymers. From the materials perspective, these donor polymers should not only have a low band gap (to increase the short circuit current, J_{sc}) but also bear a low energy level of the highest occupied molecular orbital (HOMO) (to improve the open circuit voltage, V_{oc}).[6] Typically, a low band gap polymer is designed via a "donor−acceptor" (D−A) approach, which is to incorporate electron-rich and electron-deficient moieties in the polymer backbone. The low band gap is mainly caused by the intramolecular charge transfer between donor and acceptor units.[7] Indeed, several low band gap polymers have been demonstrated with decent efficiencies (3−6%) when they were blended with PCBM or [6,6]-phenyl C_{70}-butyric acid methyl ester ($PC_{70}BM$) in typical BHJ devices.[8−28] For example, PCDTBT, a low band gap polymer synthesized from a copolymerization of alkylated carbazole and 4,7-di-2-thienyl-2,1,3-benzothiadiazole (**DTBT**), recently demonstrated a record high efficiency of 6.1% when it was blended in a BHJ composite with $PC_{70}BM$.[17]

One common feature of these successful low band gap polymers is the predominant employment of 2,1,3-benzothiadiazole (**BT**)[12,14,24] or di-2-thienyl-2,1,3-benzothiadiazole (**DTBT**)[8−10,15−17,23] as the acceptor units. Compared with the **BT** unit, **DTBT** has a few advantages. First, the two flanking thienyl units relieve the otherwise possibly severe steric hindrance between the acceptor **BT** unit and donor aromatic units (especially when benzene-based aromatics are used). Thus, the synthesized donor−acceptor polymers would adopt a more planar structure, thereby reducing the band gap by enhancing the D−A conjugation. In addition, a more planar conjugated backbone would facilitate the chain−chain interactions among polymers, improving the charge carrier (usually hole) mobility. Second, while the electron accepting **BT** unit maintains the low band gap, the two electron rich, flanking thienyl units would help improve the hole mobility, since thiophene-based polymers (such as P3HT) have shown very high hole mobility.[29] Because of these advantages,

*To whom all correspondence should be addressed. E-mail: wyou@email.unc.edu.

Published on Web 12/29/2009

the widespread usage of the **DTBT** unit has resulted in a number of polymers with high BHJ solar cell efficiencies.[8−10,15−17,20,23,30,31]

Unfortunately, the strong stacking ability of polymers incorporating the **DTBT** unit also introduces several concomitant technical difficulties. For example, the additional thiophene rings could result in polymers that are poorly soluble.[30] This low solubility can lead to low molecular weight of the polymer and unnecessary difficulty in processing the polymer. For BHJ solar cells, high molecular weight polymers are desirable, which have been shown to help enhance the efficiency of related BHJ devices, presumably by improved inter-polymer interaction to enhance the current.[32−34] Even if one could manage to obtain high molecular weight polymers, the excessive stacking may result in aggregation of polymers upon spin-casting of the film. This aggregation leads to polymer-only domains on a micrometer scale, in contrast to the desired morphology: nanometer sized, separated phases of donor polymers and fullerenes.[35] In order to fully utilize the aforementioned merits of **DTBT** units, it is important to search for new strategies to modify the structure of **DTBT** so as to improve the solubility and molecular weight of polymers incorporating **DTBT** units. In addition, such modification of **DTBT** units should also have minimum impact on the band gap and energy levels one would obtain from "conventional" polymers incorporating unmodified **DTBT** units.

There have been attempts to incorporate alkyl or alkoxy chains on the **DTBT** unit in order to enhance both the solubility and molecular weight of resulting polymers. In one study, Shi et al. copolymerized alkylated fluorene with **DTBT** modified with alkoxy chains on the 3-position of these thienyl units, resulting in a polymer with much higher molecular weight (number-average molecular weight, M_n, 68 kg/mol) and better solubility[36] than those of original polymers without any soluble chains on the **DTBT** unit.[30] However, these electron-donating alkoxy groups on the **DTBT** unit caused the HOMO level of the resulting polymer to increase, which led to a lower V_{oc}. More recently, Wang et al. attempted to add additional alkylated thiophene units to extend the **DTBT** unit.[37] The resulting D−A polymer with alkylated fluorene as the donor unit showed a smaller band gap, higher molecular weight, and better solubility compared with the original copolymer that incorporated alkylated fluorene and **DTBT** (PF-DBT).[30,38] Unfortunately, the overall efficiency of this new polymer (PFO-M3) was smaller (2.63%) than that of the original PF-D**BT** (up to 3.5%),[9] in spite of a lower band gap and a similar HOMO energy level of PFO-M3. In another study, Song et al. prepared polymers incorporating a **DTBT** unit modified with either alkyl chains on the 4-position of these thienyl units or alkoxy chains on the 3-position.[39] Compared with polymers incorporating **DTBT** without any decorated chains, these modified ones were more soluble. Again, the overall BHJ device efficiencies of polymers with such modified **DTBT** were lower than that of the corresponding **DTBT**-based polymer without alkoxy/alkyl chains, mainly due to the lower J_{sc} in the former case. Computational simulation revealed that a severe steric hindrance was introduced by these alkyl/alkoxy chains, leading to a twisted conjugated backbone in both polymers with such modified **DTBT** units.[40] Therefore, the hole mobilities of the polymers incorporating such modified **DTBT** units were noticeably lower than that of polymers with unmodified **DTBT** unit, which accounted for a smaller J_{sc} in the former case.[40] In an earlier study, Jayakannan et al. prepared the homopolymers of alkylated **DTBT** by varying alkyl chains on either 3- or 4-positions of thienyl groups.[41] Though relatively high molecular weight polymers were obtained, the steric hindrance introduced by these alkyl chains in these polymers led to much larger band gaps than that of the homopolymer of unmodified **DTBT**.[42] All these studies acknowledged the advantage of employing **DTBT** units in constructing D−A low band gap polymers for BHJ solar cells. More importantly, these previous studies underscored the importance of the functionalization of **DTBT** units to reach high molecular weight and good solubility of resulting polymers, which should lead to PV devices with higher efficiencies. Unfortunately, no improvements on BHJ devices efficiency were observed from these reported polymers that incorporated modified **DTBT** units.

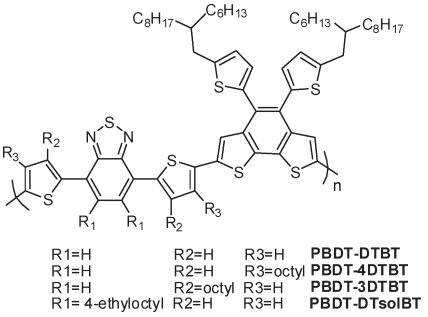

Figure 1. Chemical structures of **PBDT−DTBT**, **PBDT−4DTBT**, **PBDT−3DTBT** and **PBDT−DTsolBT**.

Previously, we have demonstrated that by incorporating a donor—bithiophene fused with a benzene moiety (benzo[2,1-*b*:3,4-*b*′]dithiophene, **BDT**)—and an acceptor—benzothiadiazole (BT)—a low band gap polymer (**PBDT−BT**) was obtained together with a low HOMO energy level.[43] However, an efficiency of only 0.6% was obtained for **PBDT−BT**, mainly due to a small J_{sc} of 2.06 mA/cm^2. This low current was ascribed to a low hole mobility (4.21×10^{-6} cm^2/(V·s)) and a low molecular weight (M_n: 10.1 kg/mol), both of which would be alleviated by introducing the modified **DTBT** units. Thus, a library of polymers incorporating **BDT** as the donor and modified **DTBT** as the acceptor unit was envisioned and synthesized (Figure 1). Alkyl chains, rather than alkoxy chains, were used to mitigate the possible elevation of the HOMO energy levels of the resulting polymers. Three variations of modified **DTBT** units were prepared: alkyl side chains at (a) the 5- and 6-positions of 2,1,3-benzothiadiazole (**DTsolBT**), (b) 3-positions of the flanking thienyl groups (**3DTBT**), and (c) 4-positions (**4DTBT**). For comparison, the polymer with unmodified **DTBT** (**PBDT-DTBT**) was also synthesized.

As expected, much higher molecular weights (~30 kg/mol) and better solubility in processing solvents were observed for all three polymers with alkylated **DTBT** units than those of **PBDT−DTBT** (9 kg/mol). Interestingly, contrary to results from previous studies, optical and electrochemical studies disclose almost identical band gap and energy levels between **PBDT−4DTBT** and **PBDT−DTBT**. These results indicate that anchoring solubilizing alkyl chains on the 4-positions of **DTBT** only introduces a minimum steric hindrance within **BDT−DTBT**, thereby maintaining the extended conjugation of the fundamental structural unit (**BDT−DTBT**). Furthermore, the polymer containing the "properly" modified **DTBT** unit, **PBDT−4DTBT**, shows an improved hole mobility of 9.2×10^{-6} cm^2/(V·s) than that of **PBDT−DTBT** (3.9×10^{-6} cm^2/(V·s)) or **PBDT−BT** (4.21×10^{-6} cm^2/(V·s)). This noticeably higher mobility of **PBDT−4DTBT**, together with its low band gap and relatively low HOMO energy level inherited from **PBDT−DTBT**, leads to a significantly improved efficiency of related BHJ solar cells (up to 2.2% has been observed), triple the efficiency obtained from BHJ devices fabricated from either **PBDT−DTBT** (0.72%) or **PBDT−BT** (0.6%).[43] A thorough investigation of this library of structurally related polymers unveils a complete picture of the influence of alkyl chains on different positions of **DTBT** units on

Scheme 1. Synthesis of Monomer A1 (Brominated DTsolBT)

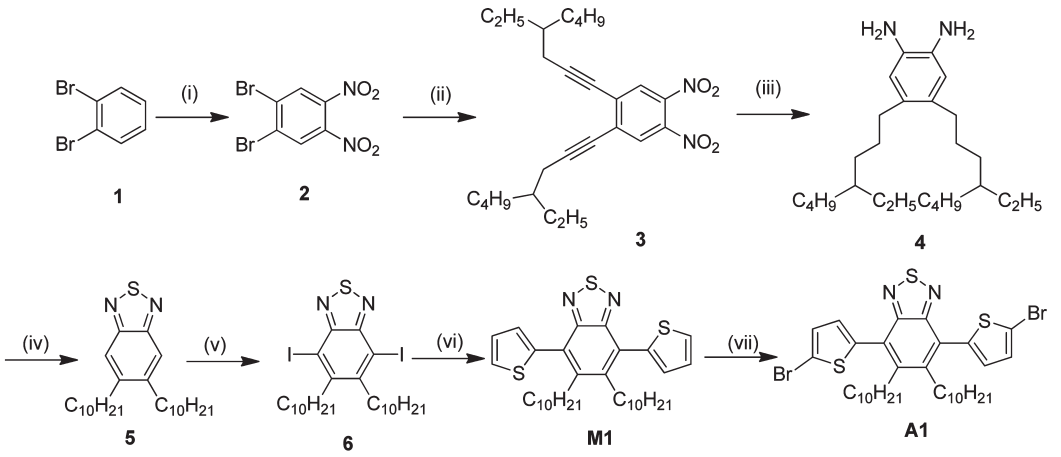

Reagents and conditions: (i) fuming H_2SO_4, fuming HNO_3, overnight; (ii) 4-ethyloct-1-yne, Et_3N, $Pd(PPh_3)_2Cl_2$, CuI, 3 h; (iii) Pd/C(10%Pd), ethyl acetate:methanol 2:1, H_2; (iv) $SOCl_2$, Et_3N, CH_2Cl_2, reflux 5 h; (v) I_2, $NaIO_3$, H_2SO_4, HOAc, H_2O, reflux overnight; (vi) thiophene,BuLi, $ZnCl_2$, 30 min; $Pd(OAc)_2$, PPh_3, THF, reflux 16 h; (vii) NBS, $CHCl_3$:HOAc=2:1, r.t, overnight

Scheme 2. Synthetic Route for A2 and A3 (Brominated 3DTBT and 4DTBT)

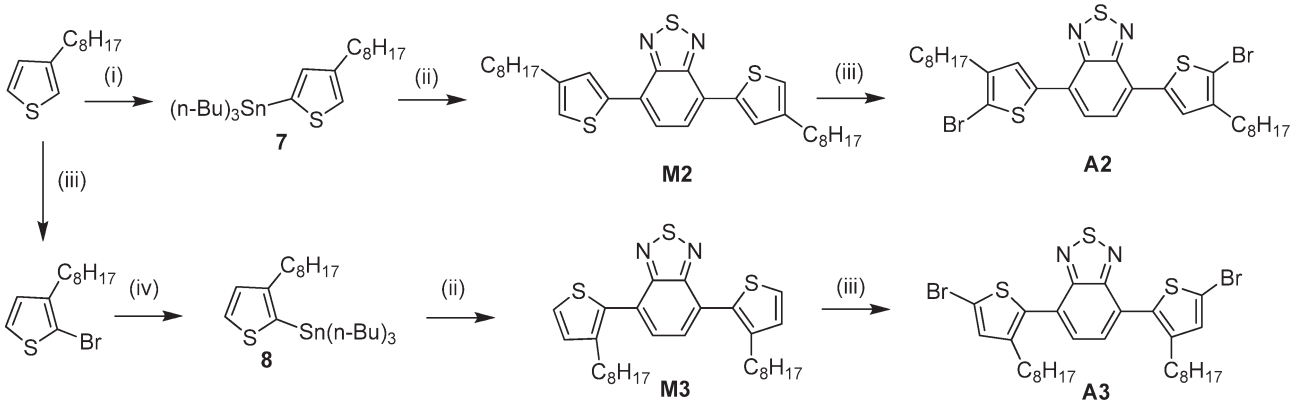

Reagents and conditions: (i) LDA, 0°C, 1 h, $(n\text{-Bu})_3SnCl$, 0°C, 30 min; (ii) $Pd(PPh_3)_2Cl_2$, THF, reflux overnight; (iii) NBS, THF, r.t. overnight; (iv) BuLi, -78°C, 2 h, $(n\text{-Bu})_3SnCl$, -78°C, 30 min

the optical, electrical, and photovoltaic properties of resulting polymers.

Results and Discussion

Monomer Synthesis. In order to obtain a high molecular weight polymer with good solubility, long, branched alkyl chains were attached at the central **BT** unit during the synthesis of **DTsolBT** (**M1** in Scheme 1). 4-Ethyloct-1-yne was prepared from commercially available 2-ethylhexyl bromide with overall yield of >60%. A Sonogashira coupling was employed to attach the 4-ethyloct-1-yne to 1,2-dibromo-4,5-dinitrobenzene (**2**) obtained by nitration of 1,2-dibromobenzene (**1**), leading to the alkylated dinitrobenzene (**3**). Both triple bonds and nitro groups were reduced simultaneously via Pd/H_2, yielding alkylated diaminobenzene (**5**). Treating (**5**) with thionyl chloride under basic conditions afforded compound (**6**), the alkylated benzothiadiazole (solBT), which then underwent several conventional halogenations and coupling reaction to monomer **A1**, the brominated **DTsolBT**.

Synthesis of **A2** and **A3** is depicted in Scheme 2. They were synthesized via slightly modified literature procedures.[41,44,45] It is worth noting that the deprotonation of 3-octylthiophene selectively occurred at the more acidic 5-position, followed by stannylation to yield (**7**). The other isomer (**8**), with tributyltin anchored at the 2-position, was obtained via 2-bromo-3-octylthiophene as the intermediate, since the bromination via NBS was selective at the more nucleophilic 2-position. Then halogen exchange with *n*-BuLi led to the lithiated 2-position, which was subsequently quenched by $(n\text{-Bu})_3SnCl$ to yield the 2-stannylated (**8**). The unmodified **DTBT** monomer was synthesized following a literature report.[46]

Polymer Synthesis. Four polymers were therefore prepared by a palladium-catalyzed Stille cross-coupling polycondensation of benzo[2,1-*b*:3,4-*b*′]dithiophene (**BDT**) distannane (**D0**) with brominated **DTBT** and its derivatives (Scheme 3). The polymerization of **PBDT−DTBT** was stopped after 18 h when precipitation was observed. The crude polymer was then precipitated from methanol and extracted via a Soxhlet apparatus with acetone, hexane, and finally chloroform. Only the chloroform-soluble portion was collected in order to obtain a high molecular weight, solution processable polymer. A noticeable amount of residue remained in the extraction thimble after the extraction with chloroform. This presumably high molecular weight portion was discarded since it would not be solution processable, which consequently led to a relatively low yield (51%)

Scheme 3. Polymerization by Stille Coupling Reaction

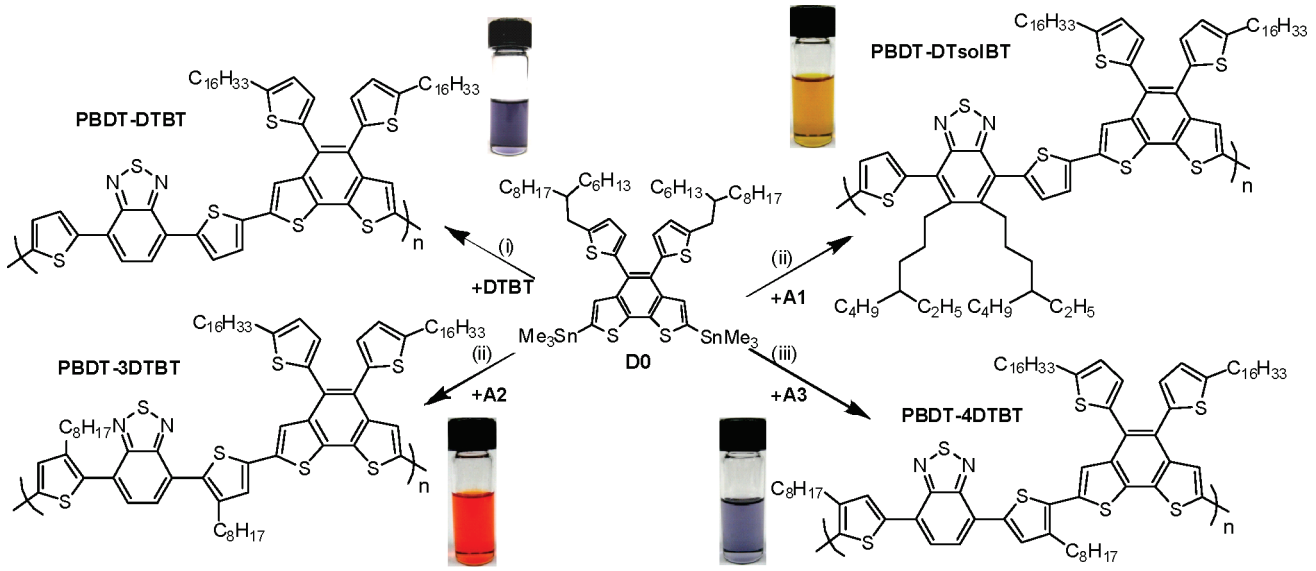

Reaction conditions: (i) Toluene, $Pd(PPh_3)_4$, reflux 24h; (ii) DMF/Toluene= 1:5, $Pd_2(dba)_3$/ P(o-tol)$_3$= 1:4, reflux 36h; (iii) Chlorobenzene, $Pd_2(dba)_3$/ P(o-tol)$_3$= 1:4, 150°C, Microwave 300W, 20min

of the polymerization. Not surprisingly, the measured molecular weight of **PBDT−DTBT** is low: the number-average (M_n) is only 9 kg/mol, and the weight-average (M_w) is 12 kg/mol, mainly due to the poor solubility of **PBDT−DTBT**.

On the other hand, adding solubilizing chains to the **DTBT** unit significantly increases the molecular weight of the resulting polymers and improves their solubility in commonly employed solvents such as THF and chloroform. Both of these features, high molecular weight and good solubility, also explain the high yields of these polymerizations even after crude polymers were extensively purified (Table 1). The structures of these purified polymers were confirmed by ^{1}H NMR and elemental analysis (Supporting Information). Neither glass transition nor melting transition was observed for all three polymers with alkylated **DTBT**, indicating the amorphous nature of these polymers. A slightly observable glass transition at ~125 °C and a barely visible melting transition at ~190 °C were obtained for **PBDT−DTBT**, partly due to its low molecular weight and more rigid backbone. Please note that microwave-assisted polymerization[47−49] was employed in synthesizing **PBDT−4DTBT**, with satisfactorily high molecular weight (comparable to that of **PBDT−3DTBT** or **PBDT−DTsolBT**) obtained in much shorter time (half an hour compared with days in conventional heating).

Optical and Electrochemical Properties. The positioning of attached solubilizing alkyl chains on the **DTBT** unit seemingly has little impact on the molecular weight and solubility of related polymers: high molecular weight and good solubility have been unanimously obtained for polymers incorporating alkylated **DTBT** units. However, dramatic effects were observed on the optical and electrochemical properties of polymers incorporating alkylated **DTBT** units, depending upon where these alkyl chains are attached on the **DTBT** units. It is surprising to discover that anchoring these alkyl chains on the 4-positions of these thienyl groups on the **DTBT** unit have negligible impact on the absorption and band gap of **PBDT−4DTBT** compared with those of **PBDT−DTBT** in solution (Figure 2a). In thin films, the unsubstituted **PBDT−DTBT** has a strong tendency to

Table 1. Polymerization Results for Polymers

	yield [%]	M_n[a] [kg/mol]	M_w[a] [kg/mol]	PDI[a]	T_d[b] [°C]
PBDT−DTBT	51	9	12	1.31	270
PBDT−4DTBT	75	27	54	1.80	420
PBDT−3DTBT	88	37	84	3.07	436
PBDT−DTsolBT	87	30	92	2.44	440

[a] Determined by GPC in tetrahydrofuran (THF) using polystyrene standards. [b] The temperature of degradation corresponding to a 5% weight loss determined by TGA at a heating rate of 10 °C/min.

π-stack: a pronounced absorption increase was observed from about 550 nm, extending up to almost 800 nm. The alkylated **PBDT−4DTBT** shows similar behavior of strong stacking, though the absorption edge is slightly blue-shifted compared with that of **PBDT−DTBT** (735 nm vs 761 nm) (Table 2), indicative of a slight steric hindrance from these extra alkyl chains in the solid state. Nevertheless, similarly small band gaps (< 1.7 eV) have been observed for both polymers. These results suggest that anchoring alkyl chains on the 4-positions of the thienyl groups (i.e., **4DTBT**) introduces minimum steric hindrance to the original conjugated backbone of **PBDT−DTBT**, maintaining the electron delocalization from D−A structures.

When these alkyl chains are located at either the 3-positions of the thienyl groups (**3DTBT**) or the 5- and 6-positions of the 2,1,3-benzothiadiazole (**DTsolBT**), severe steric hindrance is introduced between the flanking thienyl groups and the central **BT** unit. The conjugated backbone is thereby twisted at the D−A linkage, significantly affecting the effective conjugation between the donor and the acceptor (**BT**). Large band gaps were observed for these two polymers (2.21 eV for **PBDT−3DTBT** and 2.48 eV for **PBDT−DTsolBT**). The even larger band gap of **PBDT−DTsolBT** implies much stronger steric hindrance (thereby twisting of the conjugated backbone) is introduced when alkyl chains are located at the central **BT** unit. The twisting of the backbone due to the **DTsolBT** unit also explains the fact that nearly negligible stacking was observed for **PBDT−DTsolBT** in thin film, while an appreciable red shift in thin film was still observed for **PBDT−3DTBT**. Finally, both

PBDT−DTBT and **PBDT−4DTBT** are much more absorptive in the solid state than either **PBDT−3DTBT** or **PBDT−DTsolBT**: similar absorption coefficients of about 1.5×10^{-5} cm^{-1} for the former two polymers at their maximum absorption wavelength, significantly greater than those of the latter two (up to 0.9×10^{-5} cm^{-1}) at their maxima.

Probing this library of polymers with identical conjugated backbone via cyclic voltammetry provides direct evidence on how the difference in positioning these alkyl chains affects the energy levels of these related polymers. The lowest unoccupied molecular orbital (LUMO) is essentially dominated by the common acceptor unit (BT), which explains why all four polymers show similar reduction potential and LUMO energy levels (Figure 3 and Table 2). However, the HOMO energy levels disclose dramatic differences. The HOMO energy levels of **PBDT−4DTBT** and **PBDT−DTBT** differ only slightly (− 5.27 eV vs − 5.21 eV), further indicating that anchoring alkyl chains at the 4-positions of thienyl groups has almost negligible influence on the extended conjugation of the D−A polymer. The introduction of two electron rich thienyl groups to the original **PBDT−BT** increases the electron density of the conjugated backbone, leading to an elevated HOMO energy level of **PBDT−DTBT** (− 5.21 eV) compared with that of **PBDT−BT** (− 5.34 eV).[43] Shifting these alkyl chains to the 3-positions of thienyl groups (**PBDT−3DTBT**) leads to an appreciable conjugation twisting at the linkage of thienyl groups with the central **BT** unit. The apparently reduced electron delocalization renders a lowered HOMO energy level of −5.38 eV. In the case of **PBDT−DTsolBT**, a very low HOMO level of −5.69 eV was observed, strikingly similar to that of the homopolymer of **BDT** (**HMPBDT**, −5.70 eV).[43] This apparent coincidence implies that the severe steric hindrance from **DTsolBT** may disrupt the conjugation between the "donor" and the "acceptor" in **PBDT−DTsolBT**. Thus, the HOMO is essentially localized at the **BDT** unit (and partially on thienyls), which explains similar HOMO levels of **PBDT−DTsolBT** and **HMPBDT**.

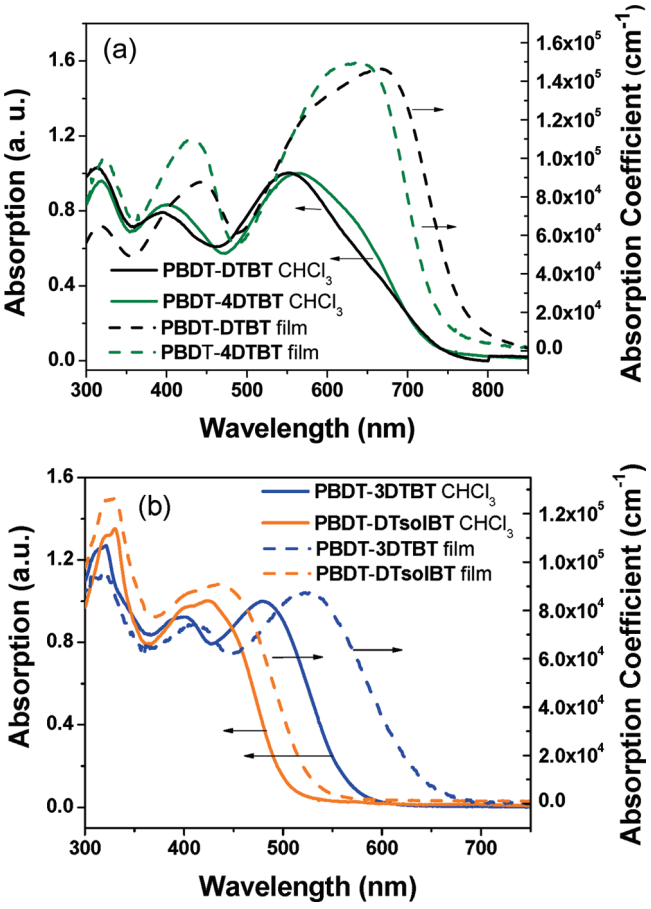

Figure 2. UV−vis spectra of all the polymers: (a) **PBDT−DTBT** and **PBDT−4DTBT** polymers in chloroform solution (solid line) and in solid film (dash line) and (b) **PBDT−DTsolBT** and **PBDT−3DTBT** polymers in chloroform solution (solid line) and in solid film (dash line).

Computational Study. Computational study of this series of polymers provides insightful information to account for the observed difference of optical and electrochemical properties. To simplify the calculation, only one repeating unit of each polymer was subject to the calculation, with alkyl chains replaced by CH_3 groups. The optimized geometry, HOMO and LUMO energy levels, and their electron density distributions were calculated at the B3LYP/6-311+G* level of theory[50,51] using density functional theory and Gaussian 03 package (Figure 4).[52]

The dihedral angles between two thienyl groups with central **BT** unit as well as the donor **BDT** unit quantitatively measure the steric hindrance introduced by these alkyl chains. All three dihedral angles for **PBDT−DTBT** are small (Table 3), indicative of complete conjugation of all

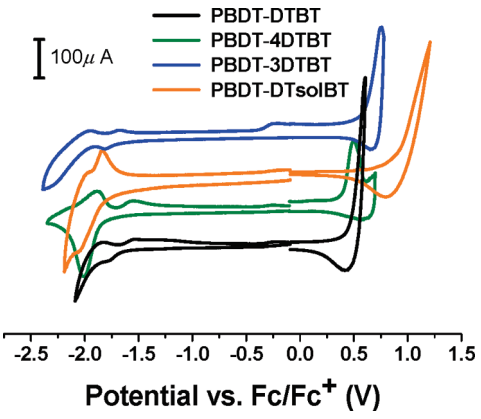

Figure 3. Cyclic voltammograms of the oxidation and reduction behavior of thin films of **PBDT−DTBT**, **PBDT−4DTBT**, **PBDT−3DTBT**, and **PBDT−DTsolBT**.

Table 2. Optical and Electrochemical Data of All Polymers

	UV−vis absorption						PL			DFT
	$CHCl_3$ solution			film			$CHCl_3$ solution	cyclic voltammetry		
polymer	λ_{max} [nm]	λ_{onset} [nm]	$E_g{}^a$ [eV]	λ_{max} [nm]	λ_{onset} [nm]	$E_g{}^a$ [eV]	λ_{max} [nm]	E^{ox}_{onset} (V)/HOMO [eV]	E^{red}_{onset} (V)/LUMO [eV]	calcd HOMO [eV]
PBDT−DTBT	550	738	1.68	666	761	1.63	628	0.47/−5.27	−1.64/−3.16	−5.22
PBDT−4DTBT	567	726	1.70	641	735	1.69	619	0.41/−5.21	−1.82/−2.98	−5.19
PBDT−3DTBT	475	560	2.21	520	628	1.97	654	0.58/−5.38	−1.67/−3.13	−5.33
PBDT−DTsolBT	425	500	2.48	435	528	2.35	580	0.89/−5.69	−1.79/−3.01	−5.43

[a] Calculated from the intersection of the tangent on the low energetic edge of the absorption spectrum with the baseline.

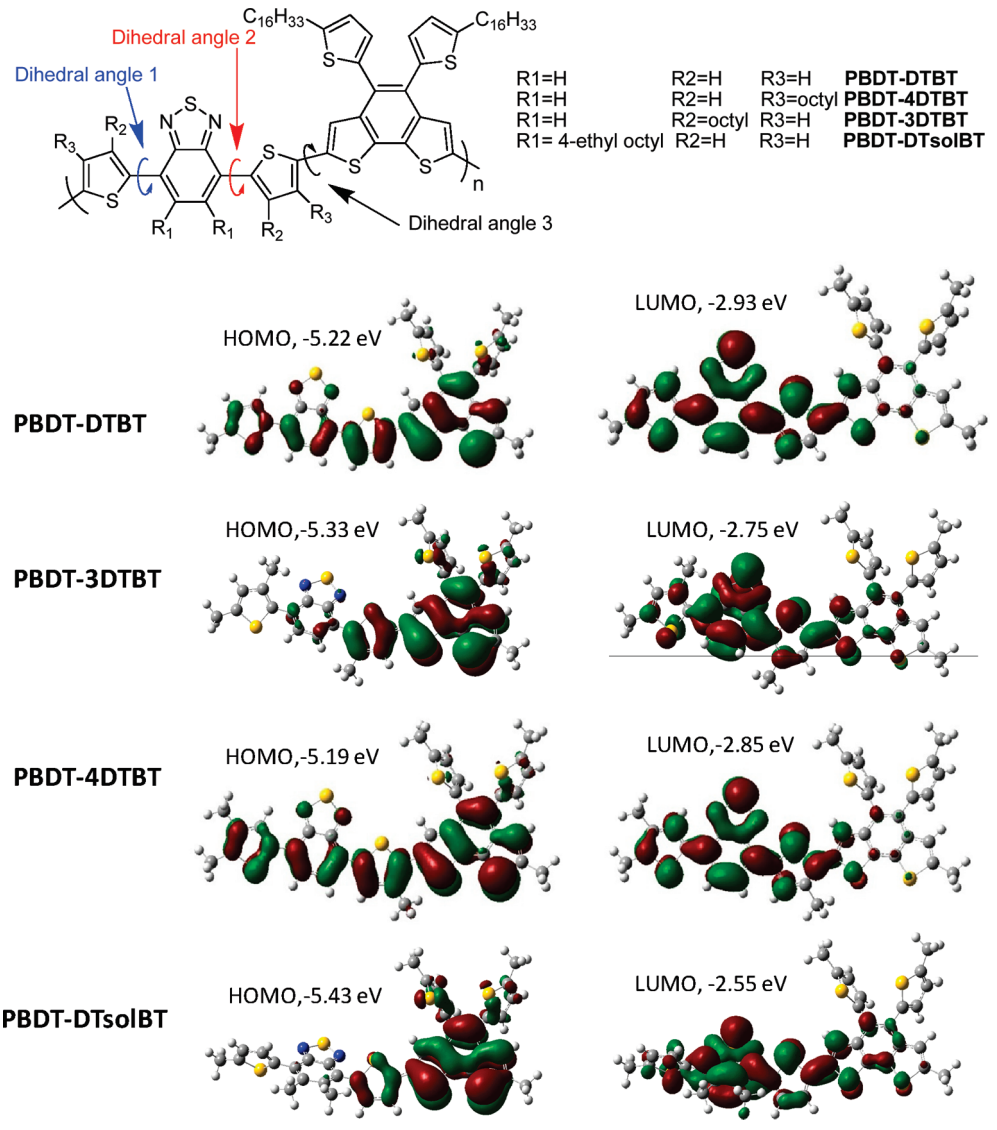

Figure 4. Calculated HOMO (left) and LUMO (right) orbitals of polymers.

participating aromatic units. The electron density is well delocalized along the conjugated backbone, as displayed by the isosurface of the HOMO energy level of **PBDT−DTBT** (Figure 4). There is only a slight increase of the dihedral angle between the 4-substituted thienyl group and **BDT** unit in **PBDT−4DTBT**, confirming the minimum steric hindrance introduced by the **4DTBT**. The electron density is also delocalized in the HOMO of **PBDT−4DTBT**, though slightly biased toward the **BDT** unit compared with that of **PBDT−DTBT**. These very similar—however slightly different—HOMO isosurfaces explain that only a slight difference (0.06 eV) was observed for the HOMO energy levels of **PBDT−DTBT** and **PBDT−4DTBT**. Furthermore, the electron density of LUMO energy levels of both **PBDT−DTBT** and **PBDT−4DTBT** are essentially localized on the **DTBT** unit, supporting observed similar LUMO energy levels. All these similarities contribute to the similar UV−vis absorptions and band gaps of **PBDT−DTBT** and **PBDT−4DTBT**.

Moving these alkyl chains away from the vicinity of **BDT** unit in the case of **PBDT−3DTBT** and **PBDT−DTsolBT** relieves the steric hindrance between substituted **DTBT** and **BDT** unit, recovering small numbers on dihedral angle 3 (Table 3). However, greater steric hindrance is formed

Table 3. Calculated Dihedral Angles of Polymers[a]

polymer	dihedral angle 1 (deg)	dihedral angle 2 (deg)	dihedral angle 3 (deg)
PBDT−DTBT	4.1	10.9	14.1
PBDT−4DTBT	5.2	14.3	30.2
PBDT−3DTBT	50.7	36.2	17.7
PBDT−DTsolBT	58.0	55.2	19.9

[a] Calculations were carried out for one repeating unit of each polymer, in gas phase, at temperature 0 K and in vacuum.

between thienyl groups and central **BT** unit, as shown by a dramatic numerical increase in dihedral angles 1 and 2. For example, over 50° angles have been calculated for the dihedral angels between thienyl groups and **BT** in **PBDT−DTsolBT**. This severe steric hindrance essentially breaks the conjugation at the linkages between thienyl groups and **BT**, thereby rendering the HOMO of PBDT−**DTsolBT** localized at the donor **BDT** unit. Compared with **PBDT−DTsolBT**, smaller torsional angles between thienyl groups and **BT** unit are calculated in the case of **PBDT−3DTBT**. Therefore, the electron density is slightly extended to the **BT** unit in the HOMO of **PBDT−3DTBT**. Comparing the isophases of all three polymers incorporating modified **DTBT** unit clearly explains why the measured HOMO energy level of

PBDT−3DTBT is between that of **PBDT−4DTBT** and that of **PBDT−DTsolBT**.

Photovoltaic Properties. Bulk heterojunction photovoltaic devices were constructed to investigate the influence on photovoltaic properties introduced by the subtle change in positioning alkyl chains. For fair comparison, care was taken during the processing to maintain similarly structured devices: (a) because this series of polymers have the identical conjugated backbone with only variations on the size and position of side chains, all polymers were blended with PCBM at 1:1 weight ratio in chloroform at 5 mg/mL; (b) identical spin rate (1100 rpm) and time (1 min) were employed to achieve similar film thicknesses. A typical fabricated solar cell has a configuration of glass/ITO/PEDOT:PSS(40 nm)/polymer:PCBM blend (~100 nm)/Ca(30 nm)/Al(70 nm) (Experimental Section). The current−voltage characteristics of solar cells based on these four polymers blended with PCBM are shown in Figure 5. Representative performance parameters of solar cells are listed in Table 4.

Because of its low solubility, **PBDT−DTBT** was dissolved into chloroform at high temperature (~60 °C). Polymers noticeably aggregated when the solution cooled. Therefore, the solution of **PBDT−DTBT** and PCBM was sonicated during cooling, which precipitated the polymer, resulting in a processable dispersion.[21] Films of **PBDT−DTBT**:PCBM are the thinnest (65 nm) among all the polymer:PCBM films, which is attributed to the low viscosity of the dispersion. A relatively low V_{oc} of 0.55 V was observed, likely due to the elevated HOMO energy level of **PBDT−DTBT** in the aggregated state. Excessive aggregation would also likely lead to form polymers-only domains so large that excitons cannot reach a donor/acceptor interface before they decay to the ground state.[53] Thus, the measured J_{sc} is only 3.53 mA/cm^2 despite the low band gap (1.63 eV) of **PBDT−DTBT**. Together with a *FF* of 0.37, an overall conversion efficiency of 0.72% is obtained for **PBDT−DTBT**. Not surprisingly, attaching these alkyl chains greatly improved the solubility of resulting polymers; however, the anchoring positions significantly impact the photovoltaic properties of related polymer-based BHJ PV cells. As discussed earlier, anchoring solubilizing chains at 4-positions of these thienyl groups (**PBDT−4DTBT**) has a minimum impact on the band gap and energy levels, compared with those of **PBDT−DTBT**. More importantly, the newly acquired solubility/processability of **PBDT−4DTBT** renders a much improved intermixing with PCBM without severe aggregation of polymers. Therefore, the BHJ solar cell of **PBDT−4DTBT**:PCBM displays a V_{oc} of 0.75 V (0.2 V higher than that of **PBDT−DTBT**-based solar cell). The low band gap (1.69 eV) leads to a much higher J_{sc} (5.92 mA/cm^2), leading to an overall efficiency of 1.83%. By applying 3% 1,8-diiodoocane as an additive into the processing solvent (chloroform) to modify the film morphology,[53,54] a higher efficiency of 2.17% is achieved, mainly due to the noticeably increased *FF* (Table 4). Adding additives appears to promote more ordering in the polymer domains, as indicated by a ~50 nm red shift in the absorption maximum of blends processed with additive (Figure 6).[55] This noticeable red shift in the absorption maximum might account for the improved J_{sc} of the devices processed with additives.

Shifting alkyl chains to the inner core of **DTBT** introduces significant steric hindrance between the aromatic units on the conjugated backbone, leading to much increased band gaps. The severe steric hindrance would also weaken the interaction between polymer chains, leading to low hole mobilities. Furthermore, the electron density of HOMO energy levels of **PBDT−3DTBT** and **PBDT−DTsolBT** are essentially localized at the **BDT** unit (Figure 4). The lack of delocalization would reduce the possibility of excitons moving to donor/acceptor interface and increase the geminate recombination of the recently dissociated excitons. Therefore, low efficiencies were observed for both **PBDT−3DTBT** (0.21%) and **PBDT−DTsolBT** (0.01%). The very small efficiency of PBDT−**DTsolBT** is largely due to severely disrupted conjugation between thienyl groups and the **BT** unit (Table 3 and Figure 4).

The BHJ devices of **PBDT−DTBT** and **PBDT−4DTBT** were further tested for their incident photon to current efficiency (IPCE). For comparison, the IPCE data are shown

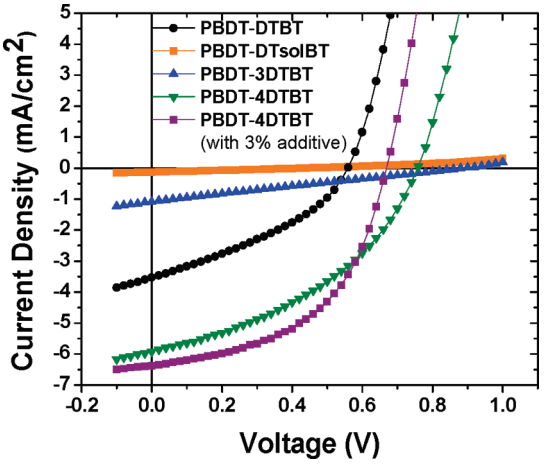

Figure 5. Characteristic *J*−*V* curves of the optimized devices of polymer-based BHJ solar cells under 1 Sun condition (100 mW/cm^2).

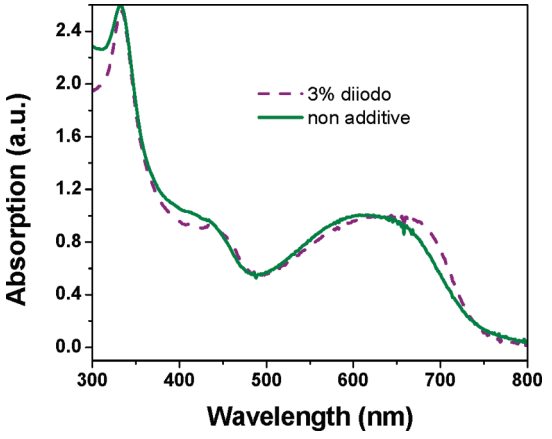

Figure 6. Comparison of absorption of **PBDT−4DTBT**:PCBM (1:1) thin films with and without additive.

Table 4. PV Performances of Polymers

polymer	polymer:PCBM	thickness (nm)	V_{oc} (V)	J_{sc} (mA/cm^2)	*FF* (%)	η (%)
PBDT−4DTBT (3% diiodooctane)	1:1	95	0.67	6.38	50.79	2.17
PBDT−4DTBT	1:1	100	0.75	5.92	41.27	1.83
PBDT−3DTBT	1:1	85	0.89	0.94	24.74	0.21
PBDT−**DTsolBT**	1:1	80	0.43	0.12	26.35	0.01
PBDT−DTBT	1:1	65	0.55	3.53	36.8	0.72

Table 5. Mobility of Polymers under SCLC Conditions

polymer only	thickness (nm)	mobility $cm^2/(V \cdot s)$	polymer:PCBM	thickness (nm)	mobility $cm^2/(V \cdot s)$
PBDT−4DTBT	55	4.36×10^{-6}	1:1 + 3% diiodooctane	75	1.60×10^{-5}
			1:1	75	9.20×10^{-6}
PBDT−DTBT	55	2.91×10^{-6}	1:1	65	3.94×10^{-6}

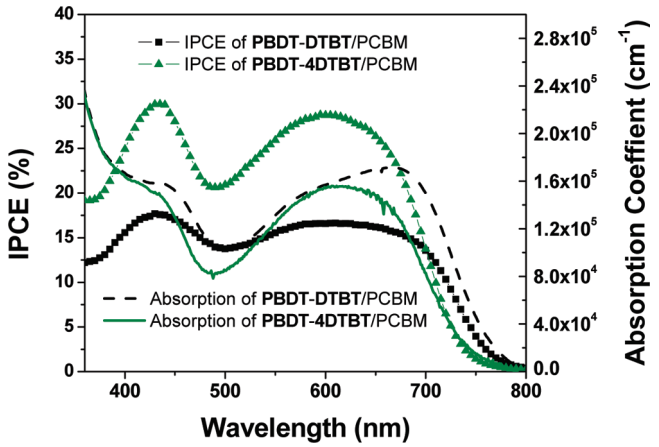

Figure 7. IPCE and absorption of **PBDT−DTBT** and **PBDT−4DTBT** (absorption is normalized by film thickness).

together with the absorption of blended thin films (Figure 7). These two films absorb light rather equally when the absorption is normalized by film thickness, though the **PBDT−DTBT** based film has slightly more absorption in the near-IR region. The IPCE curves follow individual film absorptions, with maxima at 430 and 600 nm. However, the maximum IPCE value of **PBDT−4DTBT**-based device is almost twice as much as that of **PBDT−DTBT**-based device (29% vs 16% at 600 nm). Since the film thickness of **PBDT−4DTBT**-based device is only about 50% thicker than that of **PBDT−DTBT** (100 nm vs 65 nm), these indicate that charges have much greater chance to reach the electrodes in the case of **PBDT−4DTBT**-based device, possibly due to a higher hole mobility in **PBDT−4DTBT** devices.

In order to further understand the dramatically different PV performance of these two polymers, **PBDT−DTBT** and **PBDT−4DTBT**, hole mobility values were estimated via space-charge limit current (SCLC) by fabricating hole-only devices.[56,57] For pure polymers, the measured mobilities are similar for both polymers (Table 5), with **PBDT−4DTBT** having slightly higher hole mobility. The hole mobility difference is more noticeable in the polymer/PCBM blend. The **PBDT−4DTBT**/PCBM blend demonstrates a much higher mobility, double that of the **PBDT−DTBT**/PCBM blend (Table 5). As indicated earlier, **PBDT−DTBT** has a strong tendency to stack, which is desirable in improving mobility within a polymer-only domain. However, these low molecular weight polymers, i.e., short chains, limit the interaction between different domains, leading to an overall suppressed mobility.[29] On the other hand, the properly positioned alkyl chains offer the excellent solubility and high molecular weight of **PBDT−4DTBT**. The high molecular weight of **PBDT−4DTBT** (i.e., long polymer chains) would connect locally ordered individual domains, thereby improving the hole mobility in the polymer-only devices.[58] Furthermore, the good solubility of **PBDT−4DTBT** ensures a good miscibility with PCBM in the processing solvent. The clustering of PCBM during solvent evaporation could help further aggregation of **PBDT−4DTBT** while maintaining the connection between polymer only domains, further improving the hole mobility. In addition, using additives appears to improve the film morphology with more ordering in the polymer domains, which explains an even higher hole mobility (1.60×10^{-6} $cm^2/(V\ s)$). These observations signify the importance of high molecular weight and good solubility of polymers in improving device efficiencies.

Conclusions

It has been demonstrated that introducing alkyl chains onto various positions of the dithienylbenzothiadiazole (**DTBT**) can significantly increase the molecular weight and solubility of related polymers. However, the anchoring positions of these alkyl chains have a strong influence on the optical and electrochemical properties of these structurally similar polymers with identical conjugated backbones. Contrary to previous reports, our study indicates that attaching alkyl chains on the 4-positions of these thienyl groups (i.e., **4DTBT**) only introduces minimum steric hindrance into the related D−A polymer (**PBDT−4DTBT**). Therefore, **PBDT−4DTBT** maintains almost identical band gap and energy levels compared with **PBDT−DTBT** (unmodified **DTBT**). More importantly, the additional high molecular weight and excellent solubility of **PBDT−4DTBT** lead to a more uniform mixture with PCBM, with better control on the film morphology. All these features of **PBDT−4DTBT** contribute to a much enhanced efficiency (up to 2.2%) of **PBDT−4DTBT**, significantly higher than that of **PBDT−DTBT**-based devices (0.7%). Our discovery reinforces the importance of high molecular weight and good solubility of donor polymers for BHJ solar cells, in addition to a low band gap and a low HOMO energy level, in order to further enhance the device efficiencies. Finally, we believe the strategy of "properly" modifying the acceptor unit can be applied to other D−A polymers as well. For example, 4**DTBT** can be employed in conjugation with other fused bithiophene-based polycyclic aromatics to construct D−A polymers with low band gap and low HOMO energy levels. If a higher mobility together with better controlled morphology can be achieved by these new polymers, an even higher efficiency can be expected.

Experimental Section

Reagents and Instrumentation. All reagents and chemicals were purchased from commercial sources (Aldrich, Acros, Strem, Fluka) and used without further purification unless stated otherwise. Reagent grade solvents were dried when necessary and purified by distillation. Microwave-assisted polymerizations were conducted in a CEM Discover Benchmate microwave reactor. Gel permeation chromatography (GPC) measurements were performed on a Waters 2695 separations module apparatus with a differential refractive index detector with tetrahydrofuran (THF) as eluent. The obtained molecular weight is relative to the polystyrene standard. Thermogravimetric analysis (TGA) measurements were carried out with a PerkinElmer thermogravimetric analyzer (Pyris 1 TGA) at a heating rate of 10 °C min^{-1} under a nitrogen atmosphere. The temperature of degradation (T_d) is correlated to a 5% weight loss. Differential scanning calorimetry (DSC) measurements were carried out with a model 2920 MDSC from TA Instruments under a nitrogen atmosphere. ^1H nuclear magnetic resonance (NMR) measurements were recorded either with a Bruker Avance 300 MHz AMX or a Bruker 400 MHz DRX

spectrometer. ^{13}C nuclear magnetic resonance (NMR) measurements were carried out with a Bruker 400 MHz DRX spectrometer. Chemical shifts were expressed in parts per million (ppm), and splitting patterns are designated as s (singlet), d (doublet), and m (multiplet). Coupling constants J are reported in hertz (Hz).

Electrochemistry. Cyclic voltammetry measurements were carried out using a Bioanalytical Systems (BAS) Epsilon potentiostat equipped with a standard three-electrode configuration. Typically, a three-electrode cell equipped with a glass carbon working electrode, a $Ag/AgNO_3$ (0.01 M in anhydrous acetonitrile) reference electrode, and a Pt wire counter electrode was employed. The measurements were done in anhydrous acetonitrile with tetrabutyl ammonium hexafluorophosphate (0.1 M) as the supporting electrolyte under an argon atmosphere at a scan rate of 100 mV/s. Polymer films were drop-cast onto the glassy carbon working electrode from a 2.5 mg/mL chloroform solution and dried under house nitrogen stream prior to measurements. The electrochemical onsets were determined at the position where the current starts to differ from the baseline. The potential of $Ag/AgNO_3$ reference electrode was internally calibrated by using the ferrocene/ferrocenium redox couple (Fc/Fc^+), which has a known reduction potential of -4.8 eV.[59,60] The highest occupied molecular orbital (HOMO) and lowest unoccupied molecular orbital (LUMO) energy levels of copolymers were calculated from the onset oxidation potentials (E^{ox}_{onest}) and onset reductive potentials (E^{red}_{onest}), respectively, according to eqs 1 and 2. The electrochemically determined band gaps were deduced from the difference between onset potentials from oxidation and reduction of copolymers as depicted in eq 3.

$$\text{HOMO} = -(E^{ox}_{onset} + 4.8)\ (\text{eV}) \quad (1)$$

$$\text{LUMO} = -(E^{ox}_{onset} + 4.8)\ (\text{eV}) \quad (2)$$

$$E^{EC}_{gap} = (E^{ox}_{onset} - E^{red}_{onset}) \quad (3)$$

Spectroscopy. UV−vis absorption spectra were obtained by a Shimadzu UV-2401PC spectrophotometer. Fluorescence spectra were recorded on a Shimadzu RF-5301PC spectrofluorophotometer. For the measurements of thin films, polymers were spun-coated onto precleaned glass slides from 10 mg/mL polymer solutions in chloroform. The thicknesses of films were recorded by a profilometer (Alpha-Step 200, Tencor Instruments).

Polymer Solar Cell Fabrication and Testing. Glass substrates coated with patterned indium-doped tin oxide (ITO) were purchased from Thin Film Devices, Inc. The 150 nm sputtered ITO pattern had a resistivity of 15 Ω/□. Prior to use, the substrates were ultrasonicated for 20 min in acetone followed by deionized water and then 2-propanol. The substrates were dried under a stream of nitrogen and subjected to the treatment of UV ozone over 30 min. A filtered dispersion of PEDOT:PSS in water (Baytron PH500) was then spun-cast onto clean ITO substrates at 4000 rpm for 60 s and then baked at 140 °C for 10 min to give a thin film with a thickness of 40 nm. A blend of polymer and PCBM (1:1 w/w, 10 mg/mL for polymers) was dissolved in chloroform with heating at 60 °C for 6 h. All the solutions (except in the case of **PBDT−DTBT**, which has a poor solubility) were filtered through a 0.45 μm poly(tetrafluoroethylene) (PTFE) filter and spun-cast at 1100 rpm for 60 s onto PEDOT:PSS layer. The substrates were then dried at room temperature in the glovebox under a nitrogen atmosphere for 12 h. The thicknesses of films were recorded by a profilometer (Alpha-Step 200, Tencor Instruments). The devices were finished for measurement after thermal deposition of a 30 nm film of calcium and a 70 nm aluminum film as the cathode at a pressure of $\sim 1 \times 10^{-6}$ mbar. There are eight devices per substrate, with an active area of 12 mm^2 per device. Device characterization was carried out under AM1.5G irradiation with the intensity of 100 mW/cm^2 (Oriel 91160, 300 W) calibrated by a NREL certified standard silicon cell. Current versus potential ($I-V$) curves were recorded with a Keithley 2400 digital source meter. EQE were detected under monochromatic illumination (Oriel Cornerstone 260 1/4 m monochromator equipped with Oriel 70613NS QTH lamp), and the calibration of the incident light was performed with a monocrystalline silicon diode. All fabrication steps after adding the PEDOT:PSS layer onto ITO substrate, and characterizations were performed in gloveboxes under a nitrogen atmosphere. For mobility measurements, the hole-only devices in a configuration of ITO/PEDOT:PSS (40 nm)/copolymer−PCBM/Pd (50 nm) were fabricated. The experimental dark current densities J of polymer:PCBM blends were measured when applied with voltage from 0 to 6 V. The applied voltage V was corrected from the built-in voltage V_{bi} which was taken as a compensation voltage $V_{bi} = V_{oc} + 0.05$ V and the voltage drop V_{rs} across the indium tin oxide/poly(3,4-ethylene-dioxythiophene):poly(styrenesulfonic acid) (ITO/PEDOT:PSS) series resistance and contact resistance, which is found to be around 35 Ω from a reference device without the polymer layer. From the plots of $J^{0.5}$ vs V (Supporting Information), hole mobilities of copolymers can be deduced from

$$J = \frac{9}{8}\varepsilon_r\varepsilon_0\mu_h\frac{V^2}{L^3}$$

where ε_0 is the permittivity of free space, ε_r is the dielectric constant of the polymer which is assumed to be around 3 for the conjugated polymers, μ_h is the hole mobility, V is the voltage drop across the device, and L is the film thickness of active layer.

Acknowledgment. This work was supported by the University of North Carolina at Chapel Hill, the National Science Foundation STC Program at UNC Chapel Hill (CHE-9876674), a DuPont Science and Engineering Grant, a DuPont Young Professor Award, and Office of Naval Research (Grant N000140911016).

Supporting Information Available: Synthesis of all molecules; ^1H spectra, fluorescence spectra, and DSC curves of all polymers; $J^{0.5}$ vs V plots of mobility measurement of all polymers. This material is available free of charge via the Internet at http://pubs.acs.org.

References and Notes

(1) Yu, G.; Gao, J.; Hummelen, J. C.; Wudl, F.; Heeger, A. J. *Science* **1995**, *270*, 1789.
(2) Shaheen, S. E.; Brabec, C. J.; Sariciftci, N. S.; Padinger, F.; Fromherz, T.; Hummelen, J. C. *Appl. Phys. Lett.* **2001**, *78*, 841.
(3) Ma, W. L.; Yang, C. Y.; Gong, X.; Lee, K.; Heeger, A. J. *Adv. Funct. Mater.* **2005**, *15*, 1617.
(4) Li, G.; Shrotriya, V.; Huang, J. S.; Yao, Y.; Moriarty, T.; Emery, K.; Yang, Y. *Nat. Mater.* **2005**, *4*, 864.
(5) Kim, Y.; Cook, S.; Tuladhar, S. M.; Choulis, S. A.; Nelson, J.; Durrant, J. R.; Bradley, D. D. C.; Giles, M.; McCulloch, I.; Ha, C.-S.; Ree, M. *Nat. Mater.* **2006**, *5*, 197.
(6) Scharber, M. C.; Wuhlbacher, D.; Koppe, M.; Denk, P.; Waldauf, C.; Heeger, A. J.; Brabec, C. L. *Adv. Mater.* **2006**, *18*, 789.
(7) van Mullekom, H. A. M.; Vekemans, J. A. J. M.; Havinga, E. E.; Meijer, E. W. *Mater. Sci. Eng., R* **2001**, *32*, 1.
(8) Zhang, F.; Jespersen, K. G.; Björström, C.; Svensson, M.; Andersson, M. R.; Sundström, V.; Magnusson, K.; Moons, E.; Yartsev, A.; Inganäs, O. *Adv. Funct. Mater.* **2006**, *16*, 667.
(9) Andersson, L. M.; Zhang, F.; Inganäs, O. *Appl. Phys. Lett.* **2007**, *91*, 071108.
(10) Slooff, L. H.; Veenstra, S. C.; Kroon, J. M.; Moet, D. J. D.; Sweelssen, J.; Koetse, M. M. *Appl. Phys. Lett.* **2007**, *90*, 143506.

(11) Gadisa, A.; Mammo, W.; Andersson, L. M.; Admassie, S.; Zhang, F.; Andersson, M. R.; Inganäs, O. *Adv. Funct. Mater.* **2007**, *17*, 3836.
(12) Mühlbacher, D.; Scharber, M.; Morana, M.; Zhu, Z.; Waller, D.; Gaudiana, R.; Brabec, C. *Adv. Mater.* **2006**, *18*, 2884.
(13) Zhu, Z.; Waller, D.; Gaudiana, R.; Morana, M.; Muhlbacher, D.; Scharber, M.; Brabec, C. *Macromolecules* **2007**, *40*, 1981.
(14) Peet, J.; Kim, J. Y.; Coates, N. E.; Ma, W. L.; Moses, D.; Heeger, A. J.; Bazan, G. C. *Nat. Mater.* **2007**, *6*, 497.
(15) Blouin, N.; Michaud, A.; Leclerc, M. *Adv. Mater.* **2007**, *19*, 2295.
(16) Blouin, N.; Michaud, A.; Gendron, D.; Wakim, S.; Blair, E.; Neagu-Plesu, R.; Belletete, M.; Durocher, G.; Tao, Y.; Leclerc, M. *J. Am. Chem. Soc.* **2008**, *130*, 732.
(17) Park, S. H.; Roy, A.; Beaupre, S.; Cho, S.; Coates, N.; Moon, J. S.; Moses, D.; Leclerc, M.; Lee, K.; Heeger, A. J. *Nat. Photonics* **2009**, *3*, 297.
(18) Wong, W.-Y.; Wang, X.-Z.; He, Z.; Djurisic, A. B.; Yip, C.-T.; Cheung, K.-Y.; Wang, H.; Mak, C. S. K.; Chan, W.-K. *Nat. Mater.* **2007**, *6*, 521.
(19) Liu, L.; Ho, C.-L.; Wong, W.-Y.; Cheung, K.-Y.; Fung, M.-K.; Lam, W.-T.; Djurisici, A. B.; Chan, W.-K. *Adv. Funct. Mater.* **2008**, *18*, 2824.
(20) Wu, P.-T.; Bull, T.; Kim, F. S.; Luscombe, C. K.; Jenekhe, S. A. *Macromolecules* **2009**, *42*, 671.
(21) Wienk, M. M.; Turbiez, M.; Gilot, J.; Janssen, R. A. J. *Adv. Mater.* **2008**, *20*, 2556.
(22) Chen, C.-P.; Chan, S.-H.; Chao, T.-C.; Ting, C.; Ko, B.-T. *J. Am. Chem. Soc.* **2008**, *130*, 12828.
(23) Wang, E.; Wang, L.; Lan, L.; Luo, C.; Zhuang, W.; Peng, J.; Cao, Y. *Appl. Phys. Lett.* **2008**, *92*, 033307.
(24) Hou, J.; Chen, H.-Y.; Zhang, S.; Li, G.; Yang, Y. *J. Am. Chem. Soc.* **2008**, *130*, 16144.
(25) Liang, Y.; Wu, Y.; Feng, D.; Tsai, S.-T.; Son, H.-J.; Li, G.; Yu, L. *J. Am. Chem. Soc.* **2009**, *131*, 56.
(26) Mei, J.; Ogawa, K.; Kim, Y.-G.; Heston, N. C.; Arenas, D. J.; Nasrollahi, Z.; McCarley, T. D.; Tanner, D. B.; Reynolds, J. R.; Schanze, K. S. *ACS Appl. Mater. Interfaces* **2009**, *1*, 150.
(27) Liang, Y.; Feng, D.; Wu, Y.; Tsai, S.-T.; Li, G.; Ray, C.; Yu, L. *J. Am. Chem. Soc.* **2009**, *131*, 7792.
(28) Huo, L.; Hou, J.; Chen, H.-Y.; Zhang, S.; Jiang, Y.; Chen, T. L.; Yang, Y. *Macromolecules* **2009**, *42*, 6564.
(29) Kline, R. J.; McGehee, M. D.; Kadnikova, E. N.; Liu, J.; Fréchet, J. M. J.; Toney, M. F. *Macromolecules* **2005**, *38*, 3312.
(30) Svensson, M.; Zhang, F. L.; Veenstra, S. C.; Verhees, W. J. H.; Hummelen, J. C.; Kroon, J. M.; Inganas, O.; Andersson, M. R. *Adv. Mater.* **2003**, *15*, 988.
(31) Moule, A. J.; Tsami, A.; Buennagel, T. W.; Forster, M.; Kronenberg, N. M.; Scharber, M.; Koppe, M.; Morana, M.; Brabec, C. J.; Meerholz, K.; Scherf, U. *Chem. Mater.* **2008**, *20*, 4045.
(32) Schilinsky, P.; Asawapirom, U.; Scherf, U.; Biele, M.; Brabec, C. J. *Chem. Mater.* **2005**, *17*, 2175.
(33) Ma, W.; Kim, J. Y.; Lee, K.; Heeger, A. J. *Macromol. Rapid Commun.* **2007**, *28*, 1776.
(34) Ballantyne, A. M.; Chen, L.; Dane, J.; Hammant, T.; Braun, F. M.; Heeney, M.; Duffy, W.; McCulloch, I.; Bradley, D. D. C.; Nelson, J. *Adv. Funct. Mater.* **2008**, *18*, 2373.
(35) Moon, J. S.; Lee, J. K.; Cho, S.; Byun, J.; Heeger, A. J. *Nano Lett.* **2009**, *9*, 230.
(36) Shi, C. J.; Yao, Y.; Yang, Y.; Pei, Q. B. *J. Am. Chem. Soc.* **2006**, *128*, 8980.
(37) Wang, E.; Wang, M.; Wang, L.; Duan, C.; Zhang, J.; Cai, W.; He, C.; Wu, H.; Cao, Y. *Macromolecules* **2009**, *42*, 4410.
(38) Inganäs, O.; Svensson, M.; Zhang, F.; Gadisa, A.; Persson, N. K.; Wang, X.; Andersson, M. R. *Appl. Phys. A: Mater. Sci. Process.* **2004**, *79*, 31.
(39) Song, S.; Jin, Y.; Kim, S. H.; Moon, J.; Kim, K.; Kim, J. Y.; Park, S. H.; Lee, K.; Suh, H. *Macromolecules* **2008**, *41*, 7296.
(40) Cho, S.; Seo, J. H.; Kim, S. H.; Song, S.; Jin, Y.; Lee, K.; Suh, H.; Heeger, A. J. *Appl. Phys. Lett.* **2008**, *93*, 263301.
(41) Jayakannan, M.; Van Hal, P. A.; Janssen, R. A. J. *J. Polym. Sci., Part A: Polym. Chem.* **2002**, *40*, 251.
(42) Karikomi, M.; Kitamura, C.; Tanaka, S.; Yamashita, Y. *J. Am. Chem. Soc.* **2002**, *117*, 6791.
(43) Xiao, S.; Stuart, A. C.; Liu, S.; You, W. *ACS Appl. Mater. Interfaces* **2009**, *1*, 1613.
(44) Jayakannan, M.; Van Hal, P. A.; Janssen, R. A. J. *J. Polym. Sci., Part A: Polym. Chem.* **2002**, *40*, 23602.
(45) Hou, Q.; Zhou, Q. M.; Zhang, Y.; Yang, W.; Yang, R. Q.; Cao, Y. *Macromolecules* **2004**, *37*, 6299.
(46) Zhang, C. C07D417/14 ed. U.S, **2004**; Vol. US 2004/0229925 A1.
(47) Nehls, B. S.; Asawapirom, U.; Fuldner, S.; Preis, E.; Farrell, T.; Scherf, U. *Adv. Funct. Mater.* **2004**, *14*, 352–356.
(48) Galbrecht, F.; Bunnagel, T. W.; Scherf, U.; Farrell, T. *Macromol. Rapid Commun.* **2007**, *28*, 387.
(49) Coffin, R. C.; Peet, J.; Rogers, J.; Bazan, G. C. *Nat. Chem.* **2009**, *1*, 657.
(50) Becke, A. D. *J. Chem. Phys.* **1993**, *98*, 5648.
(51) Lee, C. T.; Yang, W. T.; Parr, R. G. *Phys. Rev. B* **1988**, *37*, 785–789.
(52) Frisch, M. J.; Trucks, G. W.; Schlegel, H. B.; Scuseria, G. E.; Robb, M. A.; Cheeseman, J. R.; Montgomery J. A., Jr.; Vreven, T.; Kudin, K. N.; Burant, J. C.; Millam, J. M.; Iyengar, S. S.; Tomasi, J.; Barone, V.; Mennucci, B.; Cossi, M.; Scalmani, G.; Rega, N.; Petersson, G. A.; Nakatsuji, H.; Hada, M.; Ehara, M.; Toyota, K.; Fukuda, R.; Hasegawa, J.; Ishida, M.; Nakajima, T.; Honda, Y.; Kitao, O.; Nakai, H.; Klene, M.; Li, X.; Knox, J. E.; Hratchian, H. P.; Cross, J. B.; Adamo, C.; Jaramillo, J.; Gomperts, R.; Stratmann, R. E.; Yazyev, O.; Austin, A. J.; Cammi, R.; Pomelli, C.; Ochterski, J. W.; Ayala, P. Y.; Morokuma, K.; Voth, G. A.; Salvador, P.; Dannenberg, J. J.; Zakrzewski, V. G.; Dapprich, S.; Daniels, A. D.; Strain, M. C.; Farkas, O.; Malick, D. K.; Rabuck, A. D.; Raghavachari, K.; Foresman, J. B.; Ortiz, J. V.; Cui, Q.; Baboul, A. G.; Clifford, S.; Cioslowski, J.; Stefanov, B. B.; Liu, G.; Liashenko, A.; Piskorz, P.; Komaromi, I.; Martin, R. L.; Fox, D. J.; Keith, T.; Al-Laham, M. A.; Peng, C. Y.; Nanayakkara, A.; Challacombe, M.; Gill, P. M. W.; Johnson, B.; Chen, W.; Wong, M. W.; Gonzalez, C.; Pople, J. A. *Gaussian 03, Revision B.03*; Gaussian, Inc.: Pittsburgh, PA, 2003.
(53) Peet, J.; Senatore, M. L.; Heeger, A. J.; Bazan, G. C. *Adv. Mater.* **2009**, *21*, 1521.
(54) Lee, J. K.; Ma, W. L.; Brabec, C. J.; Yuen, J.; Moon, J. S.; Kim, J. Y.; Lee, K.; Bazan, G. C.; Heeger, A. J. *J. Am. Chem. Soc.* **2008**, *130*, 3619.
(55) Peet, J.; Cho, N. S.; Lee, S. K.; Bazan, G. C. *Macromolecules* **2008**, *41*, 8655.
(56) Melzer, C.; Koop, E. J.; Mihailetchi, V. D.; Blom, P. W. M. *Adv. Funct. Mater.* **2004**, *14*, 865.
(57) Mihailetchi, V. D.; Koster, L. J. A.; Blom, P. W. M.; Melzer, C.; de Boer, B.; van Duren, J. K. J.; Janssen, R. A. J. *Adv. Funct. Mater.* **2005**, *15*, 795.
(58) Kline, R. J.; McGehee, M. D.; Kadnikova, E. N.; Liu, J. S.; Fréchet, J. M. *J. Adv. Mater.* **2003**, *15*, 1519.
(59) Pommerehne, J.; Vestweber, H.; Guss, W.; Mahrt, R. F.; Bassler, H.; Porsch, M.; Daub, J. *Adv. Mater.* **1995**, *7*, 551.
(60) Zhan, X. W.; Liu, Y. Q.; Wu, X.; Wang, S. A.; Zhu, D. B. *Macromolecules* **2002**, *35*, 2529.